



Munich Personal RePEc Archive

**Estimating investors' behavior and errors
in probabilistic forecasts by the
Kolmogorov entropy and noise colors of
non-hyperbolic attractors**

Dominique, C-Rene

Laval University (ret.), Quebec G1K7P4, Canada

19 April 2013

Online at <https://mpra.ub.uni-muenchen.de/46451/>
MPRA Paper No. 46451, posted 22 Apr 2013 15:19 UTC

ESTIMATING INVESTORS' BEHAVIOR AND ERRORS IN PROBABILISTIC FORECASTS BY THE KOLMOGOROV ENTROPY AND NOISE COLORS OF NON-HYPERBOLIC ATTRACTORS

C-Rene Dominique*

*Professor of Applied Economics (ret.), Laval University, Quebec, Canada G1K7P4

ABSTRACT: This paper investigates the impact of the Kolmogorov-Sinai entropy on both the accuracy of probabilistic forecasts and the sluggishness of economic growth. It first posits the Gaussian process Z_t (indexed by the Hurst exponent H) as the output of a reflexive dynamic input/output system governed by a non-hyperbolic attractor. It next indexes families of attractors by the Hausdorff measure (D_0) and assesses the uncertainty level plaguing probabilistic forecast in each family. The D_0 signature of attractors is next applied to the S&P-500 Index. The result allows the construction of the dynamic history of the index and establishes robust links between the Hausdorff dimension, investors' behavior, and economic growth.

KEYWORDS: Stochastic processes, Hausdorff dimension, forecasts, entropy, attractors (strange, complex, low dimensional, chaotic), investors' behavior, economic growth.

1-INTRODUCTION

Economists and architects of financial theory have spent a considerable time studying random stochastic fields, and sequences of random variables evolving in time in the hope of finding one that would mimic the evolution of prices and or returns of financial variables. A large portion of the ensuing literature is devoted to processes such as α -stable Levy, self-similar, random walk, brownian motion with drift, and other constructed Wiener processes, etc. with particular emphasis on explaining "volatility clustering" in view of predicting the future course of financial variables. This paper is intended to show, among other things, the difficulty of reaching these objectives if one focusses solely on studying process' "characteristics" rather than on the mechanisms that drive them.

To be more specific, it is no exaggeration to say that the experts had embarked on an all-out effort to discover whether or not the property known as "long-term dependence" (LTD) exists in financial returns. LTD, another name for volatility clustering, according to Mandelbrot (1963), hinges either on specifications such as ARCH and GARCH (1 1) or on the behavior of autocorrelation functions at large lags. If the autocorrelation function is observed to decay at a geometric rate, they conclude that short-term dependence (STD) exists; whereas a decay rate that is as slow as a power law decay is assumed to reflect long-term dependence (LTD).

There are, however, a few drawbacks connected with that procedure. The nonstationarity of returns may generate spurious results that may be interpreted as LTD. When LTD and heavy tails occur together, autocorrelation functions may fail to be consistent estimators. And there exist many decay rates located between geometric and power law. Hence, the results obtained either from autocorrelation functions or from the GARCH specification do not convince because they can explain neither "market memory" nor the "dependence" of future volatility on present volatility. There are also two important omissions in the autocorrelation approach that stand to cloud the picture even further. The first is that financial time series are outputs of some "complex" dynamic systems. Even though position, behavior, and the future course of complex dynamical systems are fraught with uncertainty (see Morishima, 1976; Stokey *et al.*, 1989; Orrel, 2009, among others). there are, however, no substitutes for them. The second omission relates to the total neglect of STD, which is full of pertinent information about the state of dynamic systems, as other sciences such as seismology, acoustics, hydrology, etc. have already discovered. If markets are

dynamic constructs whose outputs (in terms of time series) vary in space and time, then variations of that nature reinforce the belief that modern markets may indeed be governed by attractors that are either “strange” or “complex” or even “chaotic”. And to shed light on the behavior of market attractors, there is no viable alternative but dynamic analyses.

This paper will steer in that direction. More specifically, the second part will be concerned with the evolution of market prices as observed outputs of complex dynamic systems while assuming that such outputs are best depicted by the so-called “fractional Brownian motion” (fBm), originally proposed by Mandelbrot and van Ness (1968), and augmented to “Mixed fractional Brownian motion” (MfBm) by Zili (2006), Thale (2009), Dominique and Rivera (2011), among others; in the MfBm process, it is easier to pinpoint the shortcomings of autocorrelation functions, for example. Part III will briefly review the salient characteristics of attracting sets, indexes, and color-codes families of attractors by the Hausdorff measure in view of assessing the extent of the Kolmogorov-Sinai entropy, assumed to be the main source of the pervasive uncertainty associated with the motion of prices. Finally, Part IV will examine the S&P-500 Index as a collection of self-affine functions in an attempt to determine whether attractors’ noise colors reflect investors’ behavior as an important determinant of economic growth.

2-THE MIXED FRACTIONAL BROWNIAN MOTION

Consider first the Mandelbrot-van Ness (1968) specification:

$$X_t^H = \{X^H(t, \omega), t \in \mathfrak{R}, \omega \in \Omega\}. \quad (1)$$

It is a real-valued intersection of self-similar and Gaussian processes defined on (Ω, Σ, P) , indexed by $H \in (0, 1)$, satisfying $E(X^H(t, \omega)) = 0, \forall t \in \mathfrak{R}$. Here, E denotes the expectation with respect to the probability law P for X^H ; (Ω, Σ) is a measurable space; H is the Hurst (1951) exponent, and X_t^H are considered non-observable inputs into the observable output Z_t given by:

$$Z_t = \sum_i b_i (X_t^{H_i}), \text{ where } b_i \in \mathfrak{R}, i \in n, H_i \in n, \forall H_i \in (0, 1), \quad (2)$$

Z_t is a linear combination of quasi self-similar Gaussian processes or a superposition of n independent input streams $(X_t^{H_i})$, each with its own H . Z_t has stationary but correlated increments, and is invariant under a whole family of transformations. As in input storage and teletraffic, $X_t^{H_i}$ is assumed to arrive into Z_t as “cars” (short-term expectations) or as “trains” (long-term expectations).

Z_t is conventionally assumed to be completely characterized by its zero mean and its covariance function, given by:

$$\text{Cov}(Z_t, Z_s) = R(t, s) = 2^{-1} \sum_i^n (b_i)^2 [t^{2H_i} + s^{2H_i} - |t-s|^{2H_i}], \quad \forall t, s \in \mathfrak{R}, i \in n. \quad (3)$$

Additionally, the probability law is interpreted as follows: Denote a positive move at time t as Δz_t^+ and a negative move as Δz_t^- . Similarly for a positive and negative moves at $t+1$ as Δz_{t+1}^+ and Δz_{t+1}^- , respectively. Next assign probability p_1 to Δz_{t+1}^+ and p_2 to Δz_{t+1}^- . Then:

$$\begin{array}{ll}
\text{Given } H > \frac{1}{2}, \text{ and } (\Delta z_t^+), \text{ then :} & p_1 (\Delta z_{t+1}^+) \gg p_2 (\Delta z_{t+1}^-) \\
H > \frac{1}{2}, \text{ and } (\Delta z_t^-) : & p_2 (\Delta z_{t+1}^-) \gg p_1 (\Delta z_{t+1}^+) \\
\text{Given } H < \frac{1}{2}, \text{ and } (\Delta z_t^+), \text{ then :} & p_2 (\Delta z_{t+1}^-) \gg p_1 (\Delta z_{t+1}^+) \\
H < \frac{1}{2}, \text{ and } (\Delta z_t^-) : & p_1 (\Delta z_{t+1}^+) \gg p_2 (\Delta z_{t+1}^-) \\
\text{Given } H = \frac{1}{2}: & p_1 = p_2 \text{ and } p_1 + p_2 = 1
\end{array} \quad (4)$$

In other words, if $H > \frac{1}{2}$ and today's move is positive, then the probability of having a positive move tomorrow (p_1) is much greater than the probability of having a negative move tomorrow (p_2). Similarly, p_2 is much greater than p_1 if today's move is negative and $H > \frac{1}{2}$, etc. However, at $H = \frac{1}{2}$, $p_1 = p_2$ is equivalent to having no useful information.

Given the conventional interpretation in (3) and (4), why then probabilistic forecasts are so wide-off their marks? To proffer an answer, consider a vector $u = [t, s]$, where $t > 0$, $s > 0$, $t > s$, and the second derivatives of (3). Denote $R_{tt} = \partial [\partial R_{t,s}] / \partial t$ and similarly for R_{ss} and $R_{ts} = R_{st}$, etc. Then:

$$\begin{array}{l}
R_{tt} = 2^{-1} \sum_i (b_i)^2 (2 H_i) (2 H_i - 1) [t^{2H_i-2} - |t-s|^{2H_i-2}] \\
R_{ss} = 2^{-1} \sum_i (b_i)^2 (2 H_i) (2 H_i - 1) [s^{2H_i-2} + |t-s|^{2H_i-2}] \\
R_{ts} = R_{st}
\end{array} \left\{ \begin{array}{l} > 0 \text{ for } H_i > \frac{1}{2} \\ = 0 \text{ for } H_i = \frac{1}{2} \\ < 0 \text{ for } H_i < \frac{1}{2} \end{array} \right. \quad (5)$$

From the Hessian matrix (\bar{H}) of (5), we have :

- i) $u^T \bar{H} u > 0$, i.e positive definite for $H_i > \frac{1}{2}$
- ii) $u^T \bar{H} u < 0$, negative definite for $H_i < \frac{1}{2}$.
- iii) $\det (\bar{H}) = 0$ for $H_i = \frac{1}{2}$,

where the T stands for the transpose operator.

Denote the autocorrelation function as $C(\tau)$, where τ is the lag, then:

$$C(\tau) = C(Z_t, Z_{t+\tau}) = [L(t, h) (1 / (\tau^{(1-2c)}))] / L(t) = 1 / (\tau^{(1-2c)}), \quad (7)$$

where $L(t, h) / L(t) \rightarrow 1$ as $t, \tau \rightarrow \infty$, $0 < c < \frac{1}{2}$, and $H_i > \frac{1}{2}$. That decay rate is observable in the *persistence* region. Whereas in the *anti-persistence* segment of H, the rate is given by:

$$C(\tau) \leq A c^\tau \text{ for } A > 0, c \in (0, 1) \text{ and } H_i < 1/2. \quad (7')$$

Equations (7) and (7') imply that for $H_i > 1/2$, $C(\tau)$ decays as a *power law* of the lag τ as t moves forward. But for $H_i < 1/2$, the autocorrelation function decays at a *geometric* rate of the lag. Further, as the determinant is zero at $H_i = 1/2$ that point is a (non-Morse) degenerate critical point of (3), indicating the exact location of a *cusp*. Put differently, for reasons that will be explicated later, (3) is in reality not strictly concave at $H_i < 1/2$ nor strictly convex at $H_i > 1/2$. Additionally, the usual assertion to the effect that a Brownian motion is recovered at $H_i = 1/2$ is not supported by (6), (7) and (7'). This is not surprising because Brownian motions are idealized and mathematically convenient intersections of *self-similar* and ∞ -*stable Levy* processes.

The above provides an explanation as to: 1) why the probability law in (4) offers so little guidance to forecasters; 2) why the jump in decay rate in (7) and (7'), and 3) why it is so difficult to come up with a convincing explanation for the presence of LTD, or volatility clustering. In fact, volatility clustering only refers to the first part of the probability law in (4), while the likelihood of high frequencies in the $H < 1/2$ region is all but ignored.

It is more promising, it seems, to focus on the signal to noise ratios, or on upper and lower bounds in information thrown-off by dynamical systems. Recalling also that statistical mechanics allows macroscopic predictions based on micro-properties of systems mediated by entropy. Then, it can be said that it is a description of how information changes as systems evolve from their initial states (Clement and Taylor, 2003; Engelberg *et al.*, 2009). And such changes are measured by the so-called Kolmogorov-Sinai entropy which, according to the Persin's Theorem (1977), may easily be evaluated by the Lyapunov characteristic exponents (LCE) or λ . Mainly for tractability, therefore, the next section briefly reviews the basic notions needed for an evaluation of information in dynamic systems.

3- CHARACTERISTICS AND NOISE COLORS OF ATTRACTING SETS

3.1 Salient Characteristics of Attractors

As already indicated, each segment of Z_t is the output of an attractor which may be strange or chaotic. As Z_t varies over time (and space) (see Kaplan and Kuo, 1993; Preciado and Morris, 2008; Baraktur *et al.*, 2003), it is essential therefore that the whole family of attractors be examined before Z_t can be completely characterized.

Let $g: \mathfrak{R}^m \rightarrow \mathfrak{R}^m$ be a diffeomorphism of a smooth global manifold, where $N(B)$ is the neighborhood of B , and $\varphi_t(B)$ is the flow or the evolution operator telling how the state of the system changes over time. If $\varphi_t(B) \subset N(\cdot)$ at $t \geq 0$ and $\varphi_t(\cdot) \rightarrow B$ as $t \rightarrow \infty$, then B is a compact *hyperbolic* attracting set for g . Moreover, in such a dissipative system, it can easily be shown that the volume of a fiducial phase space shrinks to zero as $t \rightarrow \infty$.

Next denote the locally stable and unstable manifolds for a small neighborhood of B as S and U , respectively. Next, let points in S flow forward in time, while points of U flow backward, then the globally stable and unstable manifolds of g are:

$$M^s = \cup_{t \rightarrow \infty} \varphi_t(B) \quad \text{and} \quad M^u = \cup_{t \rightarrow -\infty} \varphi_t(B).$$

These manifolds being unique and invariant under the flow, it then follows that:

$$\forall z \in M^s \lim_{t \rightarrow \infty} \varphi_t(z) = B \quad \text{and} \quad \forall z \in M^u \lim_{t \rightarrow -\infty} \varphi_t(z) = B$$

Moreover, let $\Gamma^+(z) = \{z \in \mathcal{R} | z = \varphi_t(z_0), t \geq 0\}$, and $\Gamma^-(z) = \{z \in \mathcal{R} | z = \varphi_t(z_0), t \leq 0\}$ be positive and negative half trajectories through z_0 , respectively, such that $\Gamma^+ \cup \Gamma^- = \Gamma$. Then:

$$M^s(\Gamma^+) = \cup_{t \rightarrow \infty} \varphi_t(S(\Gamma^+)) \quad \text{and} \quad M^u(\Gamma^-) = \cup_{t \rightarrow -\infty} \varphi_t(U(\Gamma^-)). \quad (8)$$

Thus, the attracting set is a “thin” set comprising two interleaved subsets of points of zero volume that do intersect. Trajectories, on the other hand, do not intersect, but they may move from M^s to M^u as they circulate.

The attractor above may be defined as *hyperbolic* in which trajectories of the saddle type, stable, and unstable manifolds are everywhere transversal. Its structure is everywhere homogeneous, and its properties are preserved under small parameter perturbations and as well under small noisy perturbations as long as the noise source is independent and uniformly distributed.

Non-hyperbolic attractors that concerns us here have smooth horse-shoe shaped manifolds that can lead to stable orbits and to transversality at the point of tangency. In hyperbolic attractors, the angle between $M^s(\cdot)$ and $M^u(\cdot)$ is bounded away from zero, but the absence of this condition leads to non-hyperbolicity with tangencies in the unstable direction. In hyperbolic attractors, expansion and contraction occur along typical trajectories, but the absence of this leads to non-hyperbolicity with unstable dimension variability.

It suffices at this point to say that most chaotic attractors are non-hyperbolic where stretching and shrinking make them strange. Kantz *et al.*, 2002 give various methods of distinguishing hyperbolic and non-hyperbolic attractors. Here, we will be concerned with the non-hyperbolic type.

There are three characteristics of non-hyperbolic attractors that are of interest here:

- 1) If the attractor is strange, it resembles a Cantor point set containing a countable subset of periodic orbits of large periods; an uncountable subset of non-periodic orbits, and a dense orbit (Dominique and Rivera, 2012);
- 2) some attractors are termed “complex”, or high dimensional chaotic, if the sum of their positive Lyapunov characteristic exponents (λ) exceeds the sum of their negative λ s but in the absence of sensitive dependence on initial conditions (SDIC). Put differently, the number of *effective* degrees of freedom of these attractors is lower than the dimension of the embedding space (m) but higher (hence Hausdorff dimension (D_0)) than that of “chaotic” attractors;
- 3) attractors that are termed “chaotic”, or low dimensional chaotic, do have SDIC, and still a lower number of effective degrees of freedom than complex attractors. This is due to the concept of self-organization whereby these attractors have managed to reduce their own entropy by discharging chunk of it to an external reservoir to satisfy the Second Law of thermodynamics.

The Hausdorff dimension of an attractor is a non-probabilistic measure of how orbits fill up the space available to them. Estimating the D_0 of segments of Z_t is therefore an easy way of identifying complex and chaotic attractors, as will be shown in the next section. But for now, let us reemphasize two points that will guide the reader for the rest of the discussion. That is, the hallmark of chaotic attractors is SDIC which may be quantified in terms of λ_s which, in turn, measure the rate of exponential divergence of nearby trajectories. The second is the concept of the Kolmogorov entropy which measures the rate of information not available in dynamic systems. The next section will use iterated function systems (IFS) to first classify attractors by broad classes, and next will attempt to estimate the level of entropy in each class.

3.2 Indexing Attractors with the Hausdorff Dimension

The easiest way to separate non-hyperbolic attractors by broad sub-classes and index them either by the Hurst exponent or the Hausdorff measure is to consider a family of Iterated Function Systems (F) (see Dominique and Rivera, 2013 and reference therein). That is,

$$F = \{f_i\}, f_i: (0, 1) \rightarrow (0, 1), i \in n, \text{ where}$$

$$f_i(z_t) = z_{t+1} = K z_t - K h z_t^{\eta+1}, \quad (9)$$

Equation (9) is quite general. Its mean (z^*), control factor (K), equilibrium (z^*) and stability condition are given by:

$$z^* = \{1/[h(\eta+1)]\}^{1/\eta}, K = 1/[z^* (1 - h z^{*\eta})], z^* = [(K - 1)/hK] \text{ and } df_i/dz_t = K [1 - h z^{\eta} (\eta + 1)] \in [-1, 1].$$

However if $h=1$ and $\eta = 1$, (9) is reduced to a modified version of Jean-Francois Verhult's growth equation, a. k.a, the logistic parabola, which is non-hyperbolic. In that form, solutions exist for $1 \leq K \leq 4$, but solutions for $1 \leq K \leq 3$ yield fixed-point attractors, while those between $3 < K \leq 4$ generate period-doubling, complex, and chaotic attractors. Another important feature to note is that every f_i between $3 < K \leq 4$ may be indexed either by $H \in (0, 1)$ or by $D_0 \in (1, 2)$, starting with the highest member, denoted f^{\max} for which $H = 0$ or $D_0 = 2$. Thus, $K = 4 - H = 2 + D_0$ describes any f in the range of D_0 and indexes its output at the same time. Equation (9) can then be written as:

$$f(z) = (2 + D_0) z_t (1 - z_t), \text{ for } h=1, \eta = 1 \quad (10)$$

The iteration process identifies attractors, beginning with the first bifurcation given by:

$$f(f(z_t)) = K \{ K z^* (1 - z^*) [1 - K z^* (1 - z^*)] \} = z^*, \quad (11)$$

but $z^* = 1/2$ is the first superstable orbit encountered ($df_i/dz = 0$) and it happens to be a member of the list of all equilibria of successive iterates. The next iterates are $f(f(f(z))) = z^*$, $f(f(f(f(z)))) = z^*$, etc. The result is such that every f_i has a D_0 signature distinguishing it from another, and each describes a prototypical attractor.

We use the Wavelet Multi-resolution Benoit_{TM} of Trusoft International to compute D_0 in the range of $3 < K \leq 4$. The result given in Figure 1 and Table 1 below allows for 5 classes of attractors according to their characteristics. The pertinent conclusions that can be drawn are as follows:

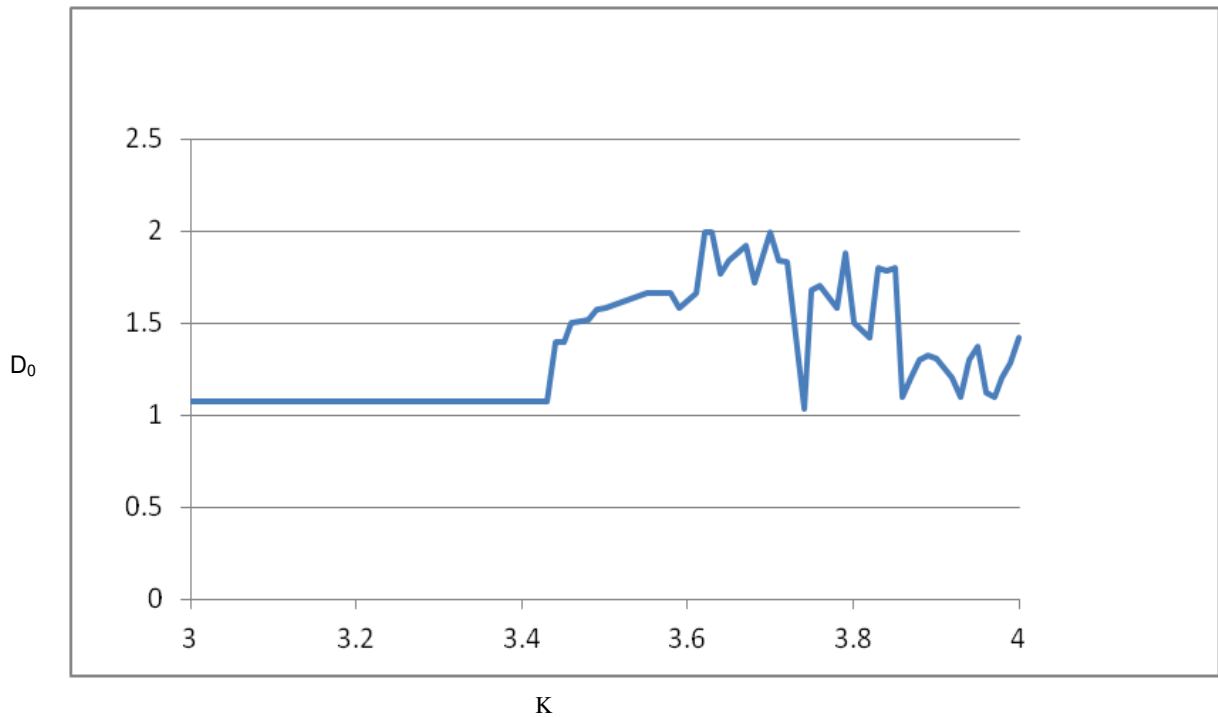


Figure 1: D_0 vs. K . Over the interval $3.0 < K < 3.44$, the process is a persistent monofractal. Over the interval $3.45 < K < 3.84$ it is an anti-persistent multifractal. The interval $3.82 \dots \leq K \leq 3.84 \dots$ is the Li & Yorke's period-3 window. The interval $3.84 < K < 4.0$ is persistent- multifractal and chaotic

Type of attractors	Range of D_0	Concentration	Power spectral density (β)	LCEs (λ)	Noise colors	Remark
Fixed-point	$1.0 < D_0 < 1.2$	---	$2.6 < \beta < 3.0$	< 0	Black	Experimentally, lower bound of D_0 is 1.08
Period-doubling	$1.41 < D_0 < 1.59$	---	$1.8 < \beta < 2.18$	< 0	Dark pink	Black band at $1.42 < D_0 < 1.47$
Fractal	$D_0 \approx 1.59$	---	$\beta \approx 1.82$	< 0	Dark pink	\approx Cantor-point set; no SDIC
Complex	$1.59 < D_0 < 2.$	$D_0 \approx 1.7$	$1.0 < \beta < 1.8$	> 0	Pink	No SDIC; high dimensional chaos
Chaotic	$1.2 < D_0 < 1.42$	$D_0 = 1.3$	$2.16 < \beta < 2.6$	> 0	Dark grey	SDIC; low-dimensional chaos

Table 1: Salient characteristics of families of attractors indexed by the Hausdorff dimension D_0 .

In one-hump maps such as (10), centered at $z = 1/2$, scale invariance should theoretically be broken at $K = 3.23$, which is a root of (11). However, as a first surprise, scale invariance is experimentally broken well after a phase shift located before the second bifurcation occurring at $K = 3.49$... The second surprise is that the lower bound of the Hausdorff measure is at $D_0 = 1.08$ rather than 1.0. Incidentally, the fact that scale invariance is broken beyond the first bifurcation explains the black band observed at the beginning of the phase of period-doubling (see Figure 2).

In *period-doubling* attractors, stable equilibria on $M^s(\cdot)$ jump to $M^u(\cdot)$ just before bifurcating. However, LCEs remain negative; a similar remark applies to the Li and York's (1975) window at $3.82 \dots \leq K \leq 3.84 \dots$

In *fractal or strange* attractors, LCEs are zero as orbits are either periodic or aperiodic, but no SDIC is observed. Consequently, there is no chaotic motion in the sense of Eckmann and Ruelle (1985).

Attractors that exhibit *complex* motion are also high-dimensional chaotic. Their D_0 is higher than those of other types, indicating thereby the *highest level of Kolmogorov-Sinai entropy*. Attractors in that family are able to decrease their entropy by dissipation. That is, they simply organize motion around fewer effective degrees of freedom by discharging entropy into an external reservoir. However, until they can self-organize themselves, the area of their attracting set visited by orbits is the largest by definition. Their average D_0 is approximately 1.7.

The family of low-dimensional *chaotic* attractors has a lower D_0 than the above category; their average D_0 is about 1.3. A good example of that type is the Henon map even though the latter is 2-dimensional and possesses a number of features that distinguish them from (10).

It is tempting at this juncture to confront these results with computed values available in the literature. It is found that complex attractors have a larger D_0 , averaging 1.7, and the *area* of the attracting set visited by orbits is also larger than *that* of chaotic attractors. For example, the complex Ikeda map:

$$x_{n+1} = 1 + 0.9 x_n \exp\{0.4i - [6i / (1 + |x_n|^2)]\}, \quad x_n, x_{n+1} \in M,$$

belongs to a family of low dimensional chaotic attractors. Its average D_0 is 1.7 and the area of the attracting set visited by orbits is larger than that of the the Henon map:

$$x_{t+1} = 1.0 + y_t - a x_t$$

$$y_{t+1} = b x_t;$$

for $a = 1.4$, and $b = 0.3$, its $D_0 = 1.3$. Moreover, the subset of B visited by orbits is much smaller than that of the Ikeda attractor. In (10) at $K = 4$, one enters into a regime of complete chaos with a $D_0 = 1.42$. Whereas in the Henon attractor, at $a > 1.55$, all orbits similarly escape to infinity.

Finally, it is hypothesized that that fractal attractors should appear as a Cantor point-set. Grassberger (1981) has carried out theoretical and analytical computations on a map such as (10) but in 1-D and has found a $D_0 = 0.538$... at aperiodicity, close to the Cantor set whose $D_0 = 0.6309$. In this study, the value found in 1-D is $0.58 < D_0 < 0.6$.

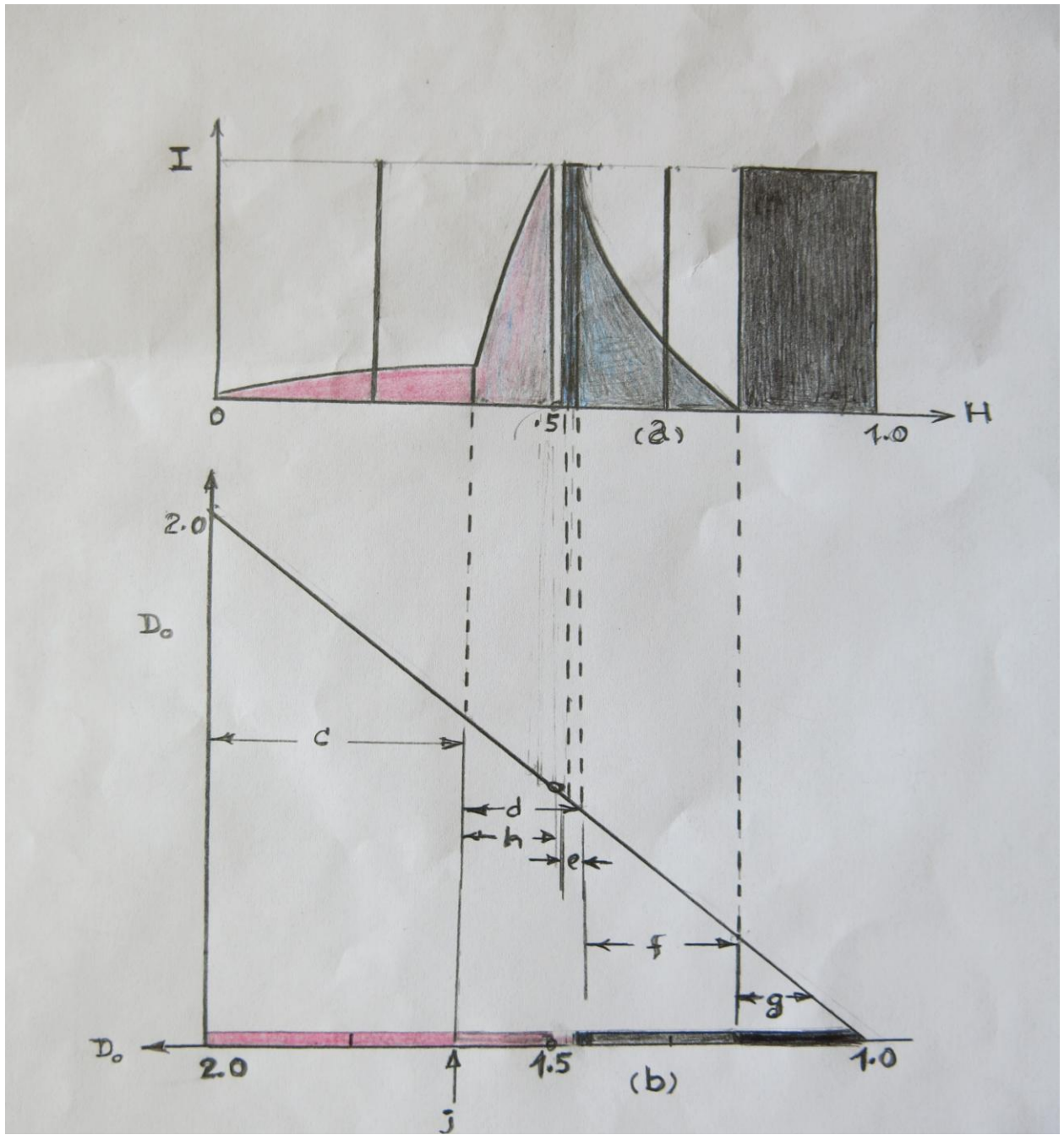


Figure 2 : Families of attractors indexed by the Hurst exponent (H) and the Hausdorff dimension (D_0). Plate (a): Information level vs. H. The depth of the valleys (white space) indicates the extent of information not available due to the Kolmogorov entropy. Plate (b): Distance c is pink; distance d is dark pink and black (e); distance f is dark grey; distance g is black, point j indicates the location of strange attractors.

3.3 Assessing the Entropy Level

The laws of physics do not permit the destruction of information. Then the Kolmogorov entropy must be interpreted as a measure of information not available. Figure 2 (Plate a) above is a sketch of the findings of Table 1. The Kolmogorov entropy is equal to the sum of positive LCEs of an attractor. The entropy of each type is presented in Plate (a) of Figure 2 as the depths of the valleys. As it can then be seen, a significant amount of entropy (or information I not available) is present in complex attractors. *This then explains why probabilistic predictions would be inadvisable for time series whose D_0 falls in the ranges of 1.6 to 2.0 and 1.2 and 1.42.* Whereas in the black regions of Figure 2, representing linearity, predictions should be a trivial matter.

4- INFORMATION, INVESTORS' BEHAVIOR, AND ECONOMIC GROWTH

As shown in Figure 2, black noise output depicts fixed-point attractors of monofractal processes. Economists call them “perfectly competitive” processes in which participants are assumed to be small but have all the market information available. The main drawback in such idealized set-ups though is the total absence of economic growth. This seems to suggest that growth is a characteristic of imperfect competition or large modern markets, but in such markets information sets of participants are necessarily incomplete. This section will show that the more incomplete the information sets of participants are (hence higher entropy) the lower is the real rate of economic growth

4.1 The Correlation of Economic growth and Investors' Behavior

This section uses the Grand Microsoft Excel data set of the S&P-500 Index, sampled daily from January 3rd 1950 to February 28th 2011. The index was first detrended using logarithmic differences and divided into 12 segments of various lengths and according to quasi self-similar scales. Each segment was next filtered for white noise. For each segment, the Hausdorff dimension (D_0) was computed using the Wavelet Multi-resolution Benoit_{TM} of Trusoft International. Next, the D_0 of each segment was matched with the average real rate of growth of the US economy over the same period. The reader should be made aware, however, that this is a coarse comparison since the series of real economic growth rates was sampled at yearly intervals. Despite this lack of sampling concordance between the series, the assertion of a correlation between investors' behavior and economic growth is borne out from at three points of view.

In teletraffic, attractors' characteristics vary with inputs' arrivals. Similarly in this study, markets characteristics vary with participants' behavior. Put differently, investors' confidence hinges information availability. The results are given in Table 2 below.

Observe first that none of the segments of the index falls within the interval $1.0 < D_0 > 1.2$. This is interpreted to mean that over the sampling period the US economy could not have been characterized by perfect competition. However, as already indicated above, scale symmetry is not broken at the expected theoretical value. Hence, when the economy was either within the interval $1.42 < D_0 < 1.47$ (black band) or within the interval $1.47 < D_0 < 1.6$ (dark pink) or the remaining of the period-doubling region, the average rate of real growth was the highest on

record. Thus, the conclusion to the effect that growth occurs when investors can rely on market information seems compelling. Further, the period-doubling region being composed of period -2 cycles, it also means that investors had no trouble “riding” these cycles, as the entropy level is low. The only exception to that rule is during the period 1972-80, when the economy was in a period of heavy inflation, i. e. in one case on twelve.

The other point of interest is that the real rates of growth appeared low when the market noise was pink. In the same vein, it is interesting to note the evolution of the average rate of growth of fixed assets over the pink region of Plate (a) of Figure 2. For example, from 2004 and 2011, private fixed assets, measured in billions of 2005 dollars, grew at an average yearly rate of 0.59 percent, while that of total fixed assets was even lower at 0.20 percent. The obvious explanation that can be found for this state of affairs is that investors’ long-term perspective was chattered by the

Period	D_0	Average Yearly Rate of Growth of Real GDP in Percent ⁽¹⁾	Noise Color
1950- 58	1.52	3.56	Dark Pink
1958-61	≈ 1.41	4.10	Dark Pink
1961-72	1.47	5.69	Black
1983-87	1.44	4.80	Black
1988-92	1.47	3.32	Black
1992-97	≈ 1.54	3.78	Dark Pink
1998-02	1.39	3.08	Dark Grey
2003-07	1.89	2.31	Pink
2007-08	≈ 1.72	0.99	Pink
2009-11	≈ 1.86	1.06	Pink
1972-80 ⁽²⁾	≈ 1.78	3.20	Pink

Table 2: Noise Color vs The average yearly rate of growth of real US GDP, 1950-2011. (1) Real US GDP in 2005 dollars from US Bureau of Economic Analysis, retrieved from www.BEA.gov on March 26th 2013. (2) Exception to the color-coded rule.

extent of the Kolmogorov entropy during that period. That also may have forced them to become “short-termists” relying more and more on high frequency trading, which seems anathema to economic growth.

Finally, Table 2 shows that at no time the market was low-dimensional-chaotic in the sense of Scheinkman and Le Baron (1989).

As hypothesized, the real rate of growth appears low when the noise is color-coded pink. If noise colors were to vary as K remains constant, such changes could be attributed to the phenomenon called “intermittency” (where stable orbits may wander into M^u before returning to M^s or due to an incomplete intersection of M^s and M^u , or even due to a reduction of effective degrees of freedom). The fact that K underwent changes rules out intermittency. In all and to

be consistent with the initial hypothesis, it seems compelling to conclude that markets are indeed *reflexive dynamic input/output constructs*.

CONCLUSIONS

This paper posits process Z_t as the output of a dynamic system whose attractor may be strange, period-doubling, complex or chaotic. When Z_t is modeled as an MfBm, it reveals the limitations of the conventional approaches used to explain volatility clustering and to predict future values of financial stochastic processes. This study instead explains volatility clustering as a matter of investors' confidence, and establishes the scaling histories of these processes in terms of the noise colors of their attractors.

In that context, iterated function systems were next used to index various sub-categories of non-hyperbolic attractors by their Hausdorff measure (D_0). As a result, it is found that the D_0 of period-doubling attractors lies between 1.41 and 1.59; that of strange attractors is about 1.59, while the average values of complex and chaotic attractors are 1.7 and 1.3, respectively. In addition, that approach allows the assessment of the Kolmogorov-Sinai entropy of each family of attractors, which appears to be the root cause of the pervasive uncertainty surrounding probabilistic forecasts.

The above results were then applied to the S&P-500 Index as a proxy for the US economy. It is found that, over the period 1950-2011 examined, the D_0 of the attractor of the economy fluctuated in values between those of period-doubling and complex. Interestingly, it is also found that the yearly real rates of economic growth were significantly higher when the noise color of the attractor was either black or dark pink rather than when it was pink. As the dynamic system in question is obviously reflexive, the paper concludes that input behavior begetting changes in attractors' noise colors is therefore a major determinant of economic growth.

REFERENCES

- Baraktur, E., Poor, V. H. and Sicar, R. K. (2003). "Estimating the fractal dimension of the S&P-500 Index using wavelet analysis". E-Quad Paper, Department of Electrical Engineering, Princeton University, Princeton, NJ 08544.
- Clements, M. P. and Taylor, N. (2003). "Evaluating internal forecasts of high-frequency financial data", *Journal of Applied Econometrics*, 18 (4), pp.415-456.
- Dominique, C-R. and Rivera, L. S. (2013). "The dynamics of market share's growth and competition in quadratic mappings", *Advances in Management & Applied Economics*, 3 (2), pp.219-235.
- (2012). "Short-term dependence in time series as an index of complexity: Examples from the S&P-500 Index", *International Business Research*, 5 (9), pp.38-48.
- ===== (2011). "Mixed fractional Brownian motion, short and long-term dependence and economic conditions", *International Business and Management*, 3 (2), pp.1-6.
- Echmann, J-P. and Ruelle, D. (1985). "Ergodic theory of chaos and strange attractors", *Review of Modern Physics*, 57, pp. 617-656.
- Engelberg, J., Manski, C. and Williams, J. (2009). "Comparing the point predictions and subjective probability distributions of professional forecasters", *Journal of Business and Economic Statistics*, 27 (1), pp.30-41.
- Grassberger, P. (1981). "On the Hausdorff dimension of fractal attractors", *Journal of Statistical Physics*, 26 (1), pp.173-179.

- Hammel, S. M., Jones, C. K. and Maloney, J. V. (1985). "Global dynamical behavior of the optical field in a ring cavity", *Journal of the Optical Society of America*, B p.2552.
- Hurst, E. H. Black, R. P. and Simaika, Y. M. (1951). "Long-term Storage: An Engineering Study", *Transactions of the American Society of Civil Engineers*, 116, pp.770-790.
- Kaplan L. M. and Jay Kuo, C. C. (1993). "Fractal estimation from noisy data via discrete fractional Gaussian noise and the Haar Basis", *IEEE Transactions*, 41, pp.3554-3562.
- Kantz, H., Grebogi, C., Awadhest, P., Ying-Cheng, L., and Sinde, E. (2002). "Unexpected robustness against noise of a class of non-hyperbolic attractors." *Physical Review E*, 65, pp.1-8.
- Li, T-Y and Yorke J. A. (1975). "Period-three implies chaos", *American Mathematical Monthly*, 82, pp.985-992.
- Mandelbrot, B. (1963). "The variation of certain speculative prices", *Journal of Business*, XXXVI, pp.392-417.
- Mandelbrot, B. and van Ness, J. W. (1968). "Fractional Brownian motion, fractional noises and applications", *SIAM Review*, 10, pp.422-427.
- Morshina, M. (1976). *The Economic Theory of Modern Society*, New York: Cambridge University Press.
- Orrel, D. (2007). *Apollo's Arrow: The Science of Prediction and the Future of Everything*, Toronto, Canada: Harper Collins.
- Pesin, Y. B. (1977). "Characteristic Lyapunov exponents and smooth Ergodic theory", *Russian Mathematical Surveys*, 32(4), pp.55-114.
- Scheinkman, J. A. and Le Baron, B. (1989). "Nonlinear dynamics and stock returns", *Journal of Business*, 62, pp.311-337.
- Sheldon, R. M. (1997). *Introduction to Probability Models*, San Diego, CA: Academic Press.
- Stokey, N. L., Lucas, R. and Prescott, E. C. (1989). *Recursive Methods in Economic Dynamics*. Cambridge, MA: Harvard University Press.
- Thale, C. (2009). "Further remarks on the mixed fractional Brownian motion", *Applied Mathematical Sciences*, 3, pp. 1-17.
- Theiler, J. (1989). "Estimating fractal dimensions", *Journal of the Optical Society of America A*, 7 (6), pp. 1056-1073.
- Zili, M. (2006). "On the mixed fractional Brownian motion", *Journal of Applied Mathematics and Statistical Analysis*, AD pp. 32435, 1-9.